A comprehensive model-assisted brain shift correction approach in image-guided neurosurgery: a case study in brain swelling and subsequent sag after craniotomy

Ma Luo*[a], Sarah F. Frisken[b], Saramati Narasimhan[a], Logan W. Clements[a],
Reid C. Thompson[c], Alexandra J. Golby[b], Michael I. Miga[a,c,d,e]

[a]Department of Biomedical Engineering, Vanderbilt University, Nashville, TN
[b]Department of Radiology, Brigham and Women's Hospital, Boston, MA
[c]Department of Neurological Surgery, Vanderbilt University Medical Center, Nashville, TN
[d]Department of Radiology, Vanderbilt University Medical Center, Nashville, TN
[e]Vanderbilt Institute for Surgery and Engineering, Vanderbilt University, Nashville, TN

ABSTRACT

Brain shift during neurosurgery can compromise the fidelity of image guidance and potentially lead to surgical error. We have developed a finite element model-based brain shift compensation strategy to correct preoperative images for improved intraoperative navigation. This workflow-friendly approach precomputes potential intraoperative deformations (a 'deformation atlas') via a biphasic-biomechanical-model accounting for brain deformation associated with cerebrospinal fluid drainage, osmotic agents, resection, and swelling. Intraoperatively, an inverse problem approach is employed to provide a combinatory fit from the atlas that best matches sparse intraoperative measurements. Subsequently, preoperative image is deformed accordingly to better reflect patient's intraoperative anatomy. While we have performed several retrospective studies examining model's accuracy using post- or intra-operative magnetic resonance imaging, one challenging task is to examine model's ability to recapture shift due to the aforementioned effects independently with clinical data and in a longitudinal manner under varying conditions. The work here is a case study where swelling was observed at the initial stage of surgery (after craniotomy and dura opening), subsequently sag was observed in a later stage of resection. Intraoperative tissue swelling and sag were captured via an optically tracked stylus by identifying cortical surface vessel features (n = 9), and model-based correction was performed for these two distinct types of brain shift at different stages of the procedure. Within the course of the entire surgery, we estimate the cortical surface experienced a deformation trajectory absolute path length of approximately 19.4 ± 2.1 mm reflecting swelling followed by sag. Overall, model reduced swelling-induced shift from 7.3 ± 1.1 to 1.8 ± 0.5 mm (~74.6% correction); for subsequent sag movement, model reduced shift from 6.4 ± 1.5 to 1.4 ± 0.5 mm (~76.6% correction).

Keywords: Brain shift, image guided surgery, neurosurgery, finite element, computational modeling

1. INTRODUCTION

The misalignment between preoperative magnetic resonance (MR) image and intraoperative patient anatomy introduced by brain shift, or soft tissue deformation of the brain, can negatively impact the quality of neurosurgical treatment, e.g. tumor margins or location of functional fiber tracts. The issue of brain shift may be addressed using intraoperative imaging techniques, such as intraoperative magnetic resonance (iMR) imaging or intraoperative ultrasound (iUS) [1,2]. Another approach to addressing brain shift is through biophysical computational modeling. The advantages and disadvantages of intraoperative imaging approaches and biophysical model-based approaches have been discussed in details in our previous work [3]. In particular here, as noted by Gerard et al., brain shift is a complex spatial-temporal event that image guidance systems that entirely rely on preoperative MR image to approach a surgical target may not be trusted over the duration of an operation [4]. Therefore it would be ideal that updated information of patient anatomy could be provided at different stages of the surgery pending the specific needs of the case [5].

In monitoring and correcting brain shift in a longitudinal manner, iMR is the clinical gold standard that offers excellent soft tissue contrast and allows comprehensive description of intraoperative shift direction and magnitude, demonstrated in Nabavi et al. [1, 6]. However, iMR acquisition increases operative time and thus making its continuous application throughout a case challenging [1, 4, 5, 7-9]. In comparison, another intraoperative imaging technique iUS, while with inferior soft tissue contrast, is more portable, economically reasonable and enables more convenient imaging acquisition intraoperatively [1, 4, 5, 7-9]. Model-based approaches attempt to bridge the gap by leveraging sparse intraoperative measurements to update high resolution preoperative MR images to account for brain shift in aiding improved neuronavigation. There is a multitude of avenues of obtaining the aforementioned sparse intraoperative measurements in a workflow-friendly fashion, such as optically tracked stylus, laser range scanning (LRS) in Sun et al. [10], stereovision in Fan et al. [11], and iUS in Morin et al. [12]. However in most studies of model-based approach in investigating brain shift compensation, the deployment of the model is often after significant resection has occurred. Understandably it is an important stage to gather valuable information such as updated patient MR image with respect to tumor margin assessment, these studies however overlook the validation effort on the temporal aspect of the brain shift problem. In recent work by Fan et al., a biomechanical model-based approach's ability to recover brain shift at two surgical stages, namely after dural opening and after partial resection, are examined [13]. This work involving 14 patients further confirms the need of repeated brain shift correction as preoperative MR image was inaccurate as soon as the dura was opened and the inaccuracy extended to resection stage [13]. While we have previously examined our model-based approach, which leverages a precomputed deformation atlas of potential brain shift estimates in the framework of an inverse problem approach, in surgery using LRS and retrospectively using iMR data, our validation effort has focused on providing brain shift correction after significant resection has been performed, yet we have not investigated the model's ability to execute repeated correction over the course of surgery [3, 10].

Furthermore, our correction strategy simulates a number of contributing factors to brain shift, e.g. gravity-induced sag from cerebrospinal fluid (CSF) drainage and swelling [10, 14]. Here in particular, swelling may be introduced by surgical trauma or physiological processes associated with tumor growth, i.e. edema [14, 15]. A study by Rasmussen et al. examined brain swelling in craniotomy procedures after opening the dura mater and found that, among 692 patients with supratentorial brain tumors, on a four-tier classification for cerebral swelling determined by the neurosurgeon (brain below the level of the dura, at the level of the dura, moderate swelling and pronounced swelling), 29.6% (205) of the studied population had moderate brain swelling and 6.1% (42) had pronounced brain swelling [16, 17]. While we have examined our model's ability to recover swelling-induced shift in Dumpuri et al. via simulation studies [18], and we have also observed the contribution of swelling solutions to the overall volumetric model brain shift estimation in a validation study performed using pre- and post- operative MR images [19], we have not probed the model's ability to correct swelling-induced shift with clinical patient data at early time points when swelling of the cortical surface is apparent within the craniotomy (i.e. in comparison, typically in past work, a very small fraction of swelling components may be utilized in analyzing brain sag). Thus in addition to the longitudinal aspect of the model validation, this work represents an in vivo case study that examines the model's performance when challenged with a scenario of brain swelling after craniotomy and dura opening at the beginning stage of a tumor resection surgery, followed by brain sag movement occurring in the later stage of the procedure. By analyzing multiple modes of deformation that occur over the temporal window of the surgery with repeated model-updated images, clinical case study reported herein presents an assessment of longitudinal application of our approach during a surgical procedure, specifically post-craniotomy and post-resection.
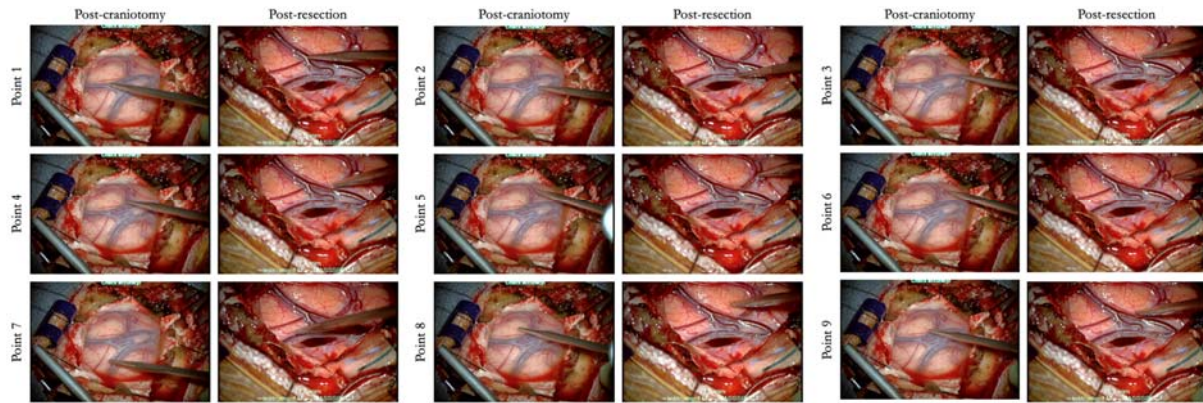
2. METHODOLOGY

2.1 Overview

This study has 3 components: (1) data acquisition; (2) deformation-atlas model-based brain shift correction; (3) qualitive and quantitative assessment of model's ability to recover brain shift due to tissue swelling and sag.
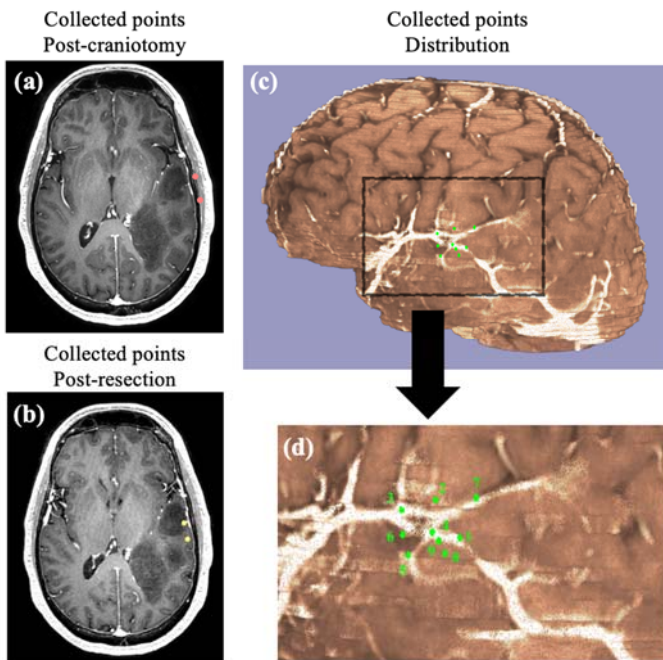
2.2 Data acquisition

Preoperatively, T1 MR image (512 x 512 x 136 with spacings of 0.51 x 0.51 x 1.00 mm) of a patient undergoing tumor resection (left temporal lobe) was acquired using Siemens 3T scanner at Brigham and Women's Hospital (Boston, Massachusetts). The approximate location and size of craniotomy were provided preoperatively [20]. Intraoperatively,

cortical surface vessel points (n = 9) were identified and collected via an optically tracked stylus. The vessel features were initially identified after craniotomy and dura opening, shown in post-craniotomy in Fig. 1. These vessel features were identified and collected again after significant resection had been performed shown in post-resection in Fig. 1. The time between two collections was ~ 2 hours. Patient consent was obtained prior to data acquisition for this IRB approved study.

Fig 1. Nine cortical surface vessel feature points acquired via an optically tracked stylus after craniotomy and dura opening, and their corresponding counterparts after resection.
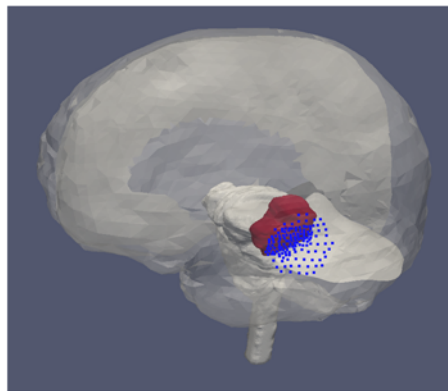
An example of the collected points (red points) after craniotomy and dura opening with the preoperative MR image registered to the patient space is shown in Fig. 2 (a), here noting the effect of swelling as the collected points are above the brain surface on the MR image. An example of the collected points (yellow points) at a later stage of the procedure after resection mapped to the preoperative MR image is shown in Fig. 2(b), here noting the effect of brain tissue sag, as the collected points are below the brain surface of the preoperative MR image. The distribution of the collected vessel points, and their spatial designation with relation to the vessel structures can be observed in the rendering of the cortical surface via FSL (FMRIB Software Library) in Fig. 2(c) and Fig. 2(d) [21-23].

Fig 2. (a) Red points indicate examples of identified and collected cortical surface vessel points via optically tracked stylus, shown on the preoperative MR image registered to the patient space at the initial stage of the resection procedure after craniotomy and dura opening. (b) Yellow points indicate examples of the collected surface features after resection shown on preoperative MR. (c) Green points indicate the points collected via optically tracked stylus, here demonstrating the spatial distribution of the collected points as well as their relation to vessel structures shown in the rendering of the cortical surface. (d) Zoom-in view of (c).

2.3 Deformation-atlas model-based brain shift correction

The brain volume and tumor volume were segmented from preoperative MR image of the patient. A surface mesh was generated from the segmented brain volume using a marching cubes algorithm followed by surface smoothing. The surface mesh was subsequently used in producing a volumetric tetrahedral mesh via a custom-build mesh generator [24]. Additionally, intensity-based rigid and non-rigid image registration techniques were utilized in transforming critical internal structures, such as brain stem, falx cerebri and tentorium cerebelli, which were expertly segmented from an atlas image volume, to patient space for patient specificity [25]. The volumetric brain mesh and the internal structures form the computation domain for our model-based approach, shown in Fig. 3, where tumor is shown in red and the craniotomy nodes are illustrated in blue.

Fig 3. Patient-specific brain mesh. Atlas brain stem, falx, and tentorium transformed to patient space via rigid and non-rigid image registrations. Craniotomy nodes are shown in blue. Tumor volume is shown in red.

Our model-based approach accounts for three distinct types of brain shift, namely gravity-induced shift, osmotic-agent-induced shift and swelling-induced shift. The displacement and boundary conditions for these simulated shifts have been detailed in our prior works [3, 10]. As one particular interest of this study is to investigate the swelling-induced shift, here briefly the displacement and pressure boundary conditions to simulate tissue swelling in our model are described: (1) brain stem was given a Dirichlet condition with no displacement and was fixed at a reference pressure; (2) the region of the craniotomy was designated as stress free, i.e. tissue is allowed to freely deform; (3) the rest of the brain surface, as well as falx and tentorium, were given slip boundary condition, which permits motion tangent to the skull along the cranial wall but no displacement in the normal direction to the surface is permitted. For the latter two conditions, the pressure condition was described with the Neumann, or no flux condition, where no drainage was permitted.

The model-based approach is built on a biphasic biomechanical model previously reported [18, 26]. In particular here, the swelling effect can be considered as the activation of elevated transfer of fluid from the capillary bed above homeostatic levels in the edematous region. This effect introduces swelling and a subsequent local tissue expansion force. To ensure that the deformation atlas approach captures the dynamic variabilities in the surgical environment, three different sizes of craniotomy, specifically 75%, 100% and 125% of the approximated size of the planned craniotomy, were simulated. Furthermore, three different capillary permeability changes allowing fluid exchange were modeled with a fixed intra-to-extra capillary pressure gradient exchange. The material properties for the brain tissue and the tumor used in this study may be found in Sun et al. [10]. With these perturbed variables, the biphasic model was solved numerically using the Galerkin weighted residual method [27]. Similarly, to achieve the deformation atlas, surgical conditions in gravity-induced shift and osmotic-agent-induced shift were perturbed according to our previous studies [3, 10]. In total, 360 gravity-induced shift solutions, 360 osmotic-agent-induced shift solutions and 9 swelling-induced shift solutions were simulated by the model and to form the deformation atlas.
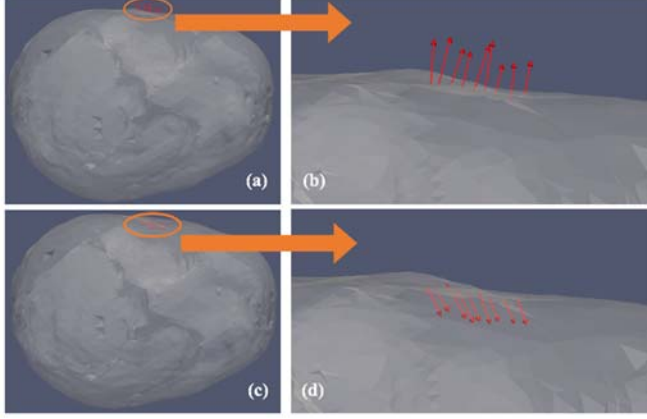
Once the deformation atlas was generated, an inverse problem approach was employed to estimate volumetric brain shift due to tissue swelling or sag. The objective of the inverse problem is to minimize the least squared error between intraoperative measurement and model prediction, where the model prediction is a combination of solutions from the deformation atlas:

$$\min\|Mw\text{-}u\|^2 \; \exists \; w_i \geq 0 \text{ and } \sum_{i=1}^{m} w_i \leq 1 \tag{1}$$

where M is the deformation atlas, w are the combinatory coefficients, and u are the measured shift. The constraints enforced on w ensure that the weighted coefficients are positive and safeguard reasonable shift estimation.

To measure shift required to drive the inverse problem approach, the vessel points collected at the initial stage of the procedure (after the craniotomy and dura opening) were projected onto the brain mesh generated from the preoperative MR image. These projected points and their stylus-collected counterparts represented the intraoperative patient anatomy change, or brain shift, due to swelling, with assumed correspondence. The measured shift due to swelling is shown in Fig.

4(a) and (b). At the later stage of the procedure after significant resection, the measured shift for brain sag deformation was obtained by examining the above projected points on the brain surface, which represents the preoperative state of the patient derived from the preoperative MR image, and their intraoperative stylus-collected counterparts, shown in Fig. 4 (c) and (d). Once the measured shift was obtained at each of the two time points of interest, a model prediction satisfying the optimization requirement of Eq (1) can be found for each condition, namely brain swelling and sag movement.

Fig 4. Intraoperative measurement of surface deformation in red vectors. (a) and (b) surface deformation due to tissue swelling. (c) and (d) surface deformation due to sag movement.

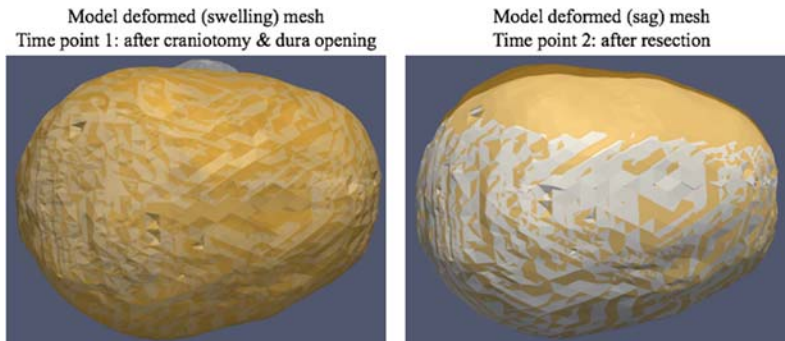## 2.4 Qualitative and quantitative assessment of model

With model prediction, the preoperative MR image can be updated to reflect patient anatomy intraoperatively due to swelling at the beginning stage of the procedure, i.e. after craniotomy and dura opening, as well as due to sag at a later stage of the surgery after resection. Additionally, the model fit is examined qualitatively and quantitatively. Specifically, for collected surface points, the intraoperative measurements shown in Fig. 4 are compared to model prediction, and the difference is defined as the residual error of the model. The percent correction in this study is further defined as:

$$\text{Percent correction} = \left(1 - \frac{e}{\|\bar{u}_{measured}\|}\right) \times 100\% \tag{2}$$

where e is the residual error defined above, $u_{measured}$ is the intraoperative measured shift, $\| \cdot \|$ is the magnitude of the shift. Lastly, a visual qualitative comparison between intraoperative measurements and model predictions is performed.

3. RESULTS

The volumetric deformation introduced by the model-based approach can be observed in Fig. 5, where the yellow mesh is generated from the preoperative MR image and the white mesh represents the model predicted shift. Particularly in Fig. 5 on the left noting the model predicted tissue swelling in the region of the craniotomy.

Model deformed (swelling) mesh
Time point 1: after craniotomy & dura opening

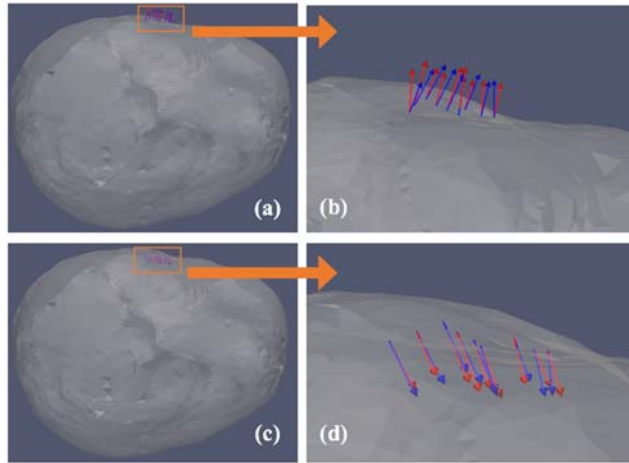Model deformed (sag) mesh
Time point 2: after resection

Fig 5. Volumetric deformation predicted by the model-based shift correction approach. (Left) At the initial stage of the procedure after dura opening, swelling-induced deformation can be observed in the craniotomy region from the yellow mesh generated from the preoperative MR to model prediction in white. (Right) At the later stage of the procedure after resection, model-predicted mesh recovering sag motion of the brain tissue illustrated in white from the yellow preoperative mesh.
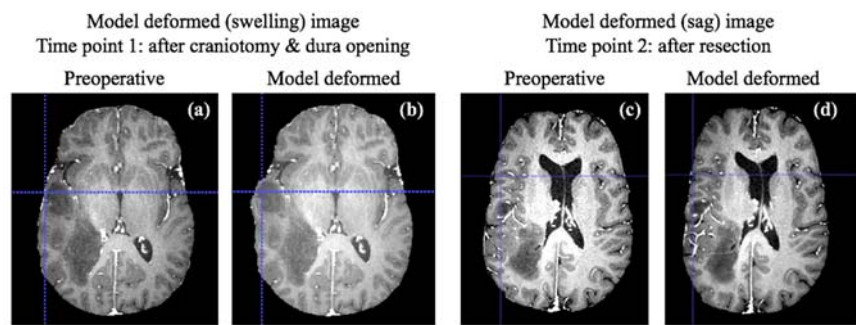
Quantitatively, for the nine collected surface vessel points, in accounting for tissue swelling after craniotomy and dura opening, the residual error after model intervention was 1.84 ± 0.48 mm from measured shift of 7.26 ± 1.11 mm, for approximately $74.6 \pm 6.6\%$ correction. In accounting for brain tissue sag, the residual error after model correction was 1.36 ± 0.50 mm from measured shift of 6.39 ± 1.48 mm, for approximately $76.6 \pm 7.8\%$ correction. Additionally, it should be noted that the time required by the inverse problem is less than 1 minute, representing minimal disruption to existing clinical workflow. It is interesting to note that the estimated path length of the cortical surface during the two deformation phases (swelling followed by the subsequent sag) was approximately 19.4 ± 2.1 mm. In previous work measuring brain shift, measurements were either focused at pulsation of the cortical surface [28] or from preoperative volume to late-stage studies [6, 29]. Recent work in the field of model-assisted system has reported swelling observations at craniotomy in the context of model-updating, but the work herein represents a more comprehensive longitudinal compensation [11]. In addition, the speed of our inverse problem approach is significantly faster: specifically, the average time to generate a whole brain deformation field is less than 1 minute in this study, in comparison it was reported to be "within 3 minutes" at the dural opening stage in that work [11].

To visualize the effect of the model, in Fig. 6 the red vectors represent the measured shift and the blue vectors represent the corresponding model prediction, demonstrating good agreement between the intraoperative measurements and model's attempt to recapture such shift due to swelling and due to tissue sag at two different time points of the surgery.
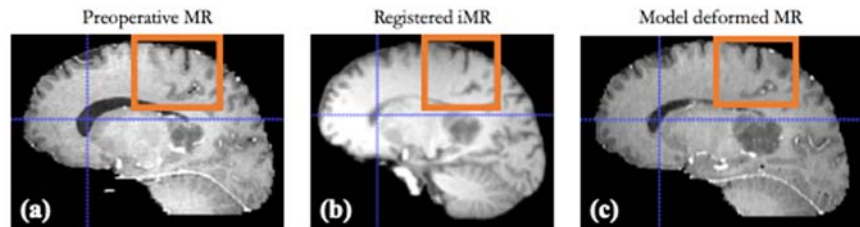

Fig 6. (a) and (b) Comparison between intraoperative measured shift (red vectors) and corresponding model predicted shift (blue vectors) in tissue swelling. (c) and (d) Comparison between intraoperative measured shift (red vectors) and corresponding model predicted shift (blue vectors) in tissue sag.

Qualitative comparisons are made between preoperative MR image of the patient and model deformed image due to swelling and sag in Fig. 7. Fig. 7(a) and (b) demonstrate the deformed MR representing model predicted swelling-induced shift compared to preoperative MR image, particularly noting in the region of craniotomy illustrated by the blue crosshair, reflecting reasonable swelling estimations representing the change of intraoperative patient anatomy. Fig. 7(c) and (d) illustrate the deformed MR representing model-predicted shift for tissue sag compared to preoperative MR, also noting the blue crosshair illustrate the change of patient anatomy on the brain surface.

Fig 7. Two qualitative comparisons between preoperative MR image (shown in (a) and (c)) and corresponding deformed MR image due to model prediction (shown in (b) for tissue swelling and (d) for tissue sag). The blue crosshair indicates intraoperative patient anatomy change due to swelling and sag on the brain surface predicted by the model when compared to the preoperative MR image.

Lastly, with the post-resection points collected before an intraoperative MR (iMR) acquisition, the model deformed image may be compared to registered iMR in Fig. 8 as an additional avenue of qualitative examination of the model performance. The orange boxes highlight better subsurface feature agreement between iMR and model deformed MR image, compared to preoperative MR. Furthermore, iMR indicates that there was a shape change at the ventricle comparing to the preoperative anatomy of the patient, which the model deformed MR was able to recapture to some extent. In particular, the blue crosshair indicate that the model was able to better depict the boundary of the ventricle.

Fig 8. Qualitative comparison between preoperative, registered intraoperative, and model deformed MR images. The orange boxes demonstrate better subsurface feature agreement between model deformed MR and intraoperative patient anatomy. The blue crosshair indicates model's ability to better describe ventricular boundary, which has altered from the preoperative to intraoperative state of the patient.

4. DISCUSSION

The work represented here is a clinical case study on the ability of a deformation-atlas model-based brain shift correction approach to recapture intraoperative shift due to swelling effect after craniotomy and dura opening followed by brain sag in one continuous case. While our previous studies have observed the contribution of the swelling solutions in the deformation atlas to the overall prediction, the model's ability to recapture shift due to tissue swelling has not been reported with clinical data. The outcome of this case study, gauged by quantitative and qualitative assessments, demonstrates that the developed model is capable of recovering shift introduced by swelling in patient data, specifically the model was able to reduce brain shift at 9 targets collected by optically tracked stylus from 7.26 ± 1.11 mm to 1.84 ± 0.48 mm for ~74.6% correction. Subsequently the model is able to resolve a second shift of tissue sag, reducing brain shift on the cortical surface measured by collected points from 6.39 ± 1.48 mm to 1.36 ± 0.50 mm for ~76.6 correction. Capturing of these modes of deformation over the course of surgery that represents a longitudinal use of the model-based approach is somewhat novel, i.e. in this work, we explore more deliberately using repeat model corrections to account for different surgical events. In this case, the events were (1) tissue swelling after craniotomy and dura opening; and (2) tissue sag after resection. Preliminary results of this study, quantitatively and qualitatively, show that with very sparse intraoperative measurements and a precomputed deformation atlas, multiple model-based brain shift estimations can be achieved to reflect dynamically changing anatomy of the patient at different time points of the neurosurgery with compelling spatial accuracy.

It also should be noted that the framework established in this work is computationally efficient and presents minimal disruption to existing clinical workflow. As mentioned previously, with a precomputed deformation atlas and a collection of surface vessel points, the inverse problem was resolved in <1 minute in generating a whole-brain deformation field prediction. In comparison, the work by Fan et al. focused on brain shift correction via a model-based approach following dural opening reported the generation of a whole-brain deformation field is "within 3 minutes" and in their follow-up work when an additional model correction was performed (after partial resection), the overall update time at that surgical stage was reported to be longer than the update time after dural opening, while in our approach the inverse problem execution time remains consistent at different time points of the surgery when brain shift correction via our model-based approach is needed [11, 13].

However, there are several aspects of the study that need further investigation. First, this study is limited in its sample size and validation targets. While the correction result at collected surface vessel points helped gauge the model performance in compensating for brain shift, independent surface and/or subsurface targets, acquired via iUS or iMR, are desired to offer further verification of model's ability of shift correction. Moreover, in future studies, we would like to extend our investigation to a larger patient population. Secondly, while collecting surface vessel points via optically tracked

stylus is one viable means of acquiring sparse intraoperative measurements to drive our model-based approach, stereovision-based approach may be another preferred method to gather said measurements as it further reduces the burden on current workflow and it offers continuous monitoring of the cortical surface [30, 31]. Lastly, while extending the examination of the model from post-resection, as we have done in our prior work, to an additional stage of post-craniotomy, strengths the confidence in our model-based approach in its temporal resolution of resolving brain shift, more surgical stages during the procedure could be further examined when the need arises to enhance the validation effort that our model-based approach can be deployed throughout the entirety of the surgery.

5. CONCLUSIONS

A case study of correcting brain shift due to tissue swelling and sag via a biophysical model-based approach at two different time points of a brain tumor resection procedure is conducted. First, as stated by Dumpuri et al., a noted shortcoming of model-updated image-guided neurosurgery system (MUIGNS) is the inability to sufficiently account for tissue swelling [18], while more cases are desired to better assess the model strategy, this study provides promising preliminary results that our biomechanical model-based approach is capable of recovering swelling conditions encountered in the operating room, with only sparse intraoperative measurements, to update preoperative imaging data for enhanced intraoperative image guidance. Secondly, the model-based approach demonstrated in this study has the potential to provide brain shift correction at different time points of interest during a surgery —an appealing aspect as brain shift is, in addition to a spatial event, a temporal phenomenon as well [4]. Lastly, this approach allows for shift correction from early time points in a procedure, which could serve to enable other image-to-physical registration strategies that may prefer to use the cortical surface for initial or repeated registrations [32].

ACKNOWLEDGEMENT

REFERENCES

1. J. M. K. Mislow, A. J. Golby, and P. M. Black, "Origins of Intraoperative MRI," *Neurosurg. Clin. N. Am.* **20**(2), 137-146 (2009).
2. U. M. Upadhyay, and A. J. Golby, "Role of pre- and intraoperative imaging and neuronavigation in neurosurgery," *Expert Rev. Med. Devices* **5**(1), 65-73 (2008).
3. M. Luo, S. F. Frisken, J. A. Weis, L. W. Clements, P. Unadkat, R. C. Thompson, A. J. Golby, and M. I. Miga, "Retrospective study comparing model-based deformation correction to intraoperative magnetic resonance imaging for image-guided neurosurgery," *J. Med. Imaging* **4**(3), 16 (2017).
4. I. J. Gerard, M. Kersten-Oertel, K. Petrecca, D. Sirhan, J. A. Hall, and D. L. Collins, "Brain shift in neuronavigation of brain tumors: A review," *Med. Image Anal.* **35**(403-420 (2017).
5. T. Arbel, X. Morandi, R. M. Comeau, and D. L. Collins, "Automatic non-linear MRI-ultrasound registration for the correction of intra-operative brain deformations AU - Arbel, Tal," *Computer Aided Surgery* **9**(4), 123-136 (2004).
6. A. Nabavi, P. M. Black, D. T. Gering, C. F. Westin, V. Mehta, R. S. Pergolizzi, M. Ferrant, S. K. Warfield, N. Hata, R. B. Schwartz, W. M. Wells, R. Kikinis, and F. A. Jolesz, "Serial intraoperative magnetic resonance imaging of brain shift," *Neurosurgery* **48**(4), 787-797 (2001).
7. C. Nimsky, O. Ganslandt, S. Cerny, P. Hastreiter, G. Greiner, and R. Fahlbusch, "Quantification of, visualization of, and compensation for brain shift using intraoperative magnetic resonance imaging," *Neurosurgery* **47**(5), 1070-1079 (2000).
8. C. Delorenzo, X. Papademetris, L. H. Staib, K. P. Vives, D. D. Spencer, and J. S. Duncan, "Image-guided intraoperative cortical deformation recovery using game theory: application to neocortical epilepsy surgery," *IEEE Trans Med Imaging* **29**(2), 322-338 (2010).

9.   E. Uhl, S. Zausinger, D. Morhard, T. Heigl, B. Scheder, W. Rachinger, C. Schichor, and J. C. Tonn, "Intraoperative Computed Tomography with Integrated Navigation System in a Multidisciplinary Operating Suite," *Neurosurgery* **64**(5), 231-239 (2009).

10.   K. Sun, T. S. Pheiffer, A. L. Simpson, J. A. Weis, R. C. Thompson, and M. I. Miga, "Near Real-Time Computer Assisted Surgery for Brain Shift Correction Using Biomechanical Models," *IEEE J Transl Eng Health Med* **2**((2014).

11.   X. Y. Fan, D. W. Roberts, T. J. Schaewe, S. B. Ji, L. H. Holton, D. A. Simon, and K. D. Paulsen, "Intraoperative image updating for brain shift following dural opening," *J. Neurosurg.* **126**(6), 1924-1933 (2017).

12.   F. Morin, H. Courtecuisse, I. Reinertsen, F. Le Lann, O. Palombi, Y. Payan, and M. Chabanas, "Brain-shift compensation using intraoperative ultrasound and constraint-based biomechanical simulation," *Med. Image Anal.* **40**(133-153 (2017).

13.   X. Y. Fan, D. W. Roberts, J. D. Olson, S. B. Ji, T. J. Schaewe, D. A. Simon, and K. D. Paulsen, "Image Updating for Brain Shift Compensation During Resection," *Operative Neurosurgery* **14**(4), 402-410 (2018).

14.   M. Ferrant, A. Nabavi, B. Macq, P. M. Black, F. A. Jolesz, R. Kikinis, and S. K. Warfield, "Serial registration of intraoperative MR images of the brain," *Med. Image Anal.* **6**(4), 337-359 (2002).

15.   S. Narasimhan, M. I. Miga, N. Rana, H. B. Johnson, A. Attia, and J. A. Weis, "Differentiating tumor recurrence from radiation-induced necrosis: An image-based mathematical modeling framework," *2018 IEEE 15th International Symposium on Biomedical Imaging (ISBI 2018)* 839-842 (2018).

16.   M. Rasmussen, H. Bundgaard, and G. E. Cold, "Craniotomy for supratentorial brain tumors: risk factors for brain swelling after opening the dura mater," *J. Neurosurg.* **101**(4), 621-626 (2004).

17.   M. Rasmussen, and G. E. Cold, "Subdural Intracranial Pressure and Degree of Swelling After Opening of Dura in Patients with Supratentorial Tumours," in *Monitoring of Cerebral and Spinal Haemodynamics During Neurosurgery* G. E. Cold, and N. Juul, Eds., pp. 103-114, Springer Berlin Heidelberg, Berlin, Heidelberg (2008).

18.   P. Dumpuri, R. C. Thompson, B. M. Dawant, A. Cao, and M. I. Miga, "An atlas-based method to compensate for brain shift: preliminary results," *Med Image Anal* **11**(2), 128-145 (2007).

19.   P. Dumpuri, R. C. Thompson, A. Cao, S. Ding, I. Garg, B. M. Dawant, and M. I. Miga, "A fast and efficient method to compensate for brain shift for tumor resection therapies measured between preoperative and postoperative tomograms," *IEEE Trans Biomed Eng* **57**(6), 1285-1296 (2010).

20.   R. C. Vijayan, R. C. Thompson, L. B. Chambless, P. J. Morone, L. He, L. W. Clements, R. H. Griesenauer, H. Kang, and M. I. Miga, "Android application for determining surgical variables in brain-tumor resection procedures," *J. Med. Imaging* **4**(1), 12 (2017).

21.   S. M. Smith, M. Jenkinson, M. W. Woolrich, C. F. Beckmann, T. E. J. Behrens, H. Johansen-Berg, P. R. Bannister, M. De Luca, I. Drobnjak, D. E. Flitney, R. K. Niazy, J. Saunders, J. Vickers, Y. Y. Zhang, N. De Stefano, J. M. Brady, and P. M. Matthews, "Advances in functional and structural MR image analysis and implementation as FSL," *Neuroimage* **23**(S208-S219 (2004).

22.   M. W. Woolrich, S. Jbabdi, B. Patenaude, M. Chappell, S. Makni, T. Behrens, C. Beckmann, M. Jenkinson, and S. M. Smith, "Bayesian analysis of neuroimaging data in FSL," *Neuroimage* **45**(1), S173-S186 (2009).

23.   M. Jenkinson, C. F. Beckmann, T. E. Behrens, M. W. Woolrich, and S. M. Smith, "FSL," *Neuroimage* **62**(2), 782-790 (2012).

24.   J. M. Sullivan, G. Charron, and K. D. Paulsen, "A three-dimensional mesh generator for arbitrary multiple material domains," *Finite Elem. Anal. Des.* **25**(3-4), 219-241 (1997).

25.   G. K. Rohde, A. Aldroubi, and B. M. Dawant, "The adaptive bases algorithm for intensity-based nonrigid image registration," *IEEE Trans Med Imaging* **22**(11), 1470-1479 (2003).

26.   M. I. Miga, K. D. Paulsen, J. M. Lemery, S. D. Eisner, A. Hartov, F. E. Kennedy, and D. W. Roberts, "Model-updated image guidance: Initial clinical experiences with gravity-induced brain deformation," *IEEE Trans. Med. Imaging* **18**(10), 866-874 (1999).

27.   D. R. Lynch, *Numerical partial differential equations for environmental scientists and engineers : a first practical course*, Springer, New York (2005).

28.   S. B. Ji, X. Y. Fan, D. W. Roberts, and K. D. Paulsen, "Cortical Surface Strain Estimation Using Stereovision," *Medical Image Computing and Computer-Assisted Intervention, Miccai 2011, Pt I* **6891**(412-+ (2011).

29.   D. W. Roberts, A. Hartov, F. E. Kennedy, M. I. Miga, and K. D. Paulsen, "Intraoperative brain shift and deformation: A quantitative analysis of cortical displacement in 28 cases," *Neurosurgery* **43**(4), 749-758 (1998).

30.   X. C. Yang, L. W. Clements, M. Luo, S. Narasimhan, R. C. Thompson, B. M. Dawant, and M. I. Miga, "Stereovision-based integrated system for point cloud reconstruction and simulated brain shift validation," *J. Med. Imaging* **4**(3), 9 (2017).

31.   A. N. Kumar, M. I. Miga, T. S. Pheiffer, L. B. Chambless, R. C. Thompson, and B. M. Dawant, "Persistent and automatic intraoperative 3D digitization of surfaces under dynamic magnifications of an operating microscope," *Med Image Anal* **19**(1), 30-45 (2015).

32.   M. I. Miga, T. K. Sinha, D. M. Cash, R. L. Galloway, and R. J. Weil, "Cortical surface registration for image-guided neurosurgery using laser-range scanning," *IEEE Trans Med Imaging* **22**(8), 973-985 (2003).